Effect of nanoparticle deposition on rewetting temperature and quench velocity in experiments with stainless steel rodlets and nanofluids

Proceedings of the Seventh International ASME Conference on Nanochannels, Microchannels and Minichannels
ICNMM2009
June 22-24, 2009, Pohang, South Korea

ICNMM2009-82082

EFFECT OF NANOPARTICLE DEPOSITION ON REWETTING TEMPERATURE AND QUENCH VELOCITY IN EXPERIMENTS WITH STAINLESS STEEL RODLETS AND NANOFLUIDS

H. Kim*, J. Buongiorno, L. W. Hu, T. McKrell
Massachusetts Institute of Technology
Cambridge, MA 02139, USA, hdkim@mit.edu

ABSTRACT

Quenching of small stainless steel rods in pure water and nanofluids with alumina and diamond nanoparticles at low concentrations (0.1 vol%) was investigated experimentally. The rods were heated to an initial temperature of ~1000 °C and then plunged into the test fluid. The results show that the quenching behavior of the nanofluids is nearly identical to that of pure water. However, due to nanofluids boiling during the quenching process, some nanoparticles deposit on the surface of the rod, which results in much higher quenching rate in subsequent tests with the same rod. It is likely that particle deposition destabilizes the film-boiling vapor film at high temperature, thus causing the quenching process to accelerate, as evident from the values of the quench front speed measured by means of a high-speed camera. The acceleration strongly depends on the nanoparticle material used, i.e., the alumina nanoparticles on the surface significantly improve the quenching, while the diamond nanoparticles do not. The possible mechanisms responsible for the quench front acceleration are discussed. It is found that the traditional concept of conduction-controlled quenching cannot explain the acceleration provided by the nanoparticle layer on the surface.

NOMENCLATURE

Bi	Biot number (=ρc/k)
c	Specific heat (J/kg-K)
f	Correction factor for wettability
h	Heat transfer coefficient (W/m^2-K)
k	Thermal conductivity (W/m-K)
q″	Heat flux (W/m^2)
R	Radius of rodlet (m)
t	Time (s)
T	Temperature (°C)
T_c	Critical temperature of water (°C)
T_{int}	Interface temperature (°C)
T_{MAX}	Maximum temperature of liquid phase (°C)
T_{MFB}	Minimum film boiling temperature (°C)
T_{rew}	Rewetting temperature (°C)
T_{rod}	Temperature of rod specimen (°C)
T*	Dimensionless temperature, $(T_{rod} - T_f)/(T_{rew} - T_f)$
u	Propagation velocity of quench front (m/sec)
vol%	Volume percent
ΔT_{sat}	Wall superheat (°C)

Greek Letter

ρ	Density (kg/m^3)
ξ	Thermal effusivity (W/m^2-K)

Subscripts

f	Fluid
sat	Saturated
w	Wall

INTRODUCTION

A number of recent investigations on boiling of nanofluids showed that such engineered fluids can effectively delay departure from nucleate boiling (DNB) with respect to pure fluids (You et al., 2003; Vassallo et al., 2004). It was found that the DNB heat flux enhancement is closely related to nanoparticle deposition, which may change the heater surface roughness significantly (Bang and Chang, 2005; Kim et al., 2006). Moreover, the deposition of oxide nanoparticles like alumina and titania significantly enhances the affinity, or wettability, of the liquid to the surface (Kim et al., 2007). These surface changes alter the boiling heat transfer characteristics, e.g., they increase the value of the critical heat flux.

Park et al. (2004) performed quenching experiments of a copper sphere in alumina nanofluids to investigate the effect of the nanoparticles on film boiling heat transfer. Their results showed that the film-boiling heat transfer rate in nanofluids was somewhat lower than in pure water. However, they observed

an intriguing phenomenon: after quenching a sphere in nanofluids, they repeated the test with the same sphere, and found that the sphere would quench much more rapidly, apparently bypassing the film boiling mode altogether. This result suggested that nanoparticle deposition on the sphere surface prevents formation of a stable vapor film, which consequently promotes a more rapid quenching. Later, some investigations were carried out by Xue et al. (2007), Choo et al. (2008), Kim et al. (2008) with similar results; however, the mechanism by which nanoparticle deposition accelerates the quenching process is not clearly understood yet.

To investigate the effect of nanofluids/nanoparticles on the quenching phenomena, we conducted quenching experiments with stainless steel rodlets in water and nanofluids. These experiments, their results and interpretation are reported in the present paper.

NANOFLUIDS PREPARATION AND PROPERTIES

We selected nanofluids with alumina nanoparticles, as this material is widely used in previous investigations of nanofluid boiling heat transfer, and also resulted in considerable enhancement of the critical heat flux. Also, diamond nanoparticles were selected to explore the effect of a material with very different physico-chemical properties. Water-based nanofluids of these two materials were purchased from Nyacol (alumina) and PlasmaChem (diamond). Nanofluids with low nanoparticle concentrations (0.1vol%) were prepared by diluting the concentrated nanofluid purchased from the vendors with distilled water.

The size of the nanoparticles in the dilute nanofluids was measured with the dynamic light scattering technique, and the averaged diameter was found to be ~39 nm for alumina and ~165 nm for diamond, respectively. The surface tension, thermal conductivity and viscosity of the nanofluids were measured by means of a Sigma 703 tensiometer, a KD2 thermal conductivity probe and a capillary viscometer, respectively. All the nanofluid properties were found to be within ±5% of those of pure water, which is not surprising, given the low concentration of nanoparticles used in our experiments.

EXPERIMENTAL DESCRIPTION

Figure 1 shows the details of the test specimen for the quenching experiments. A test specimen consists of a stainless steel rodlet (50 mm in length and 4.8 mm in diameter), a 0.5 mm-diameter K-type sheathed ungrounded thermocouple to record the temperature at the center of the rodlet, and a reinforcing precision tube to mechanically support them. The reinforcing tube is connected to a 9.5 mm-diameter connecting tube via a tube fitting.

The quenching experimental facility consists of a radiant furnace, an air slide, a quench pool, and a data acquisition system. The test specimen is preheated to ~1030°C in the furnace. Then the test specimen is quickly plunged from the furnace into the pool of the test fluid, which is maintained at atmospheric pressure and subcooled temperature of 30 or 80°C. The quench pool is a 95 × 95 mm^2 rectangular vessel having depth of 150 mm, which has an effectively infinite thermal capacity with respect to the test specimen. The pool temperature is controlled by a programmable digital hot plate. The temperature history of the inserted thermocouple at the center of the specimen is recorded using a HP Agilent 34980A data acquisition system at a rate of 10 Hz. Furthermore, the quenching process is recorded by a high speed video camera (Phantom v7.2). Further details regarding the quench facility can be found in a previous paper (Kim et al., 2008).

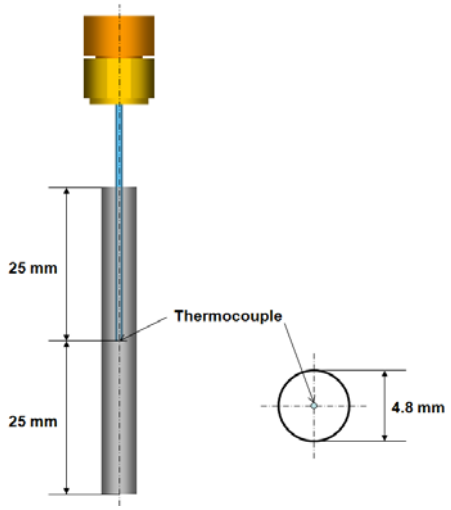

Figure 1 Schematics of the rodlet specimens

EXPERIMENTAL RESULTS

Transient cooling curve

Figure 2 shows the temperature histories of the rodlet specimens during repeated quenching tests in water, alumina and diamond nanofluids. Repetition of the quenching test in water produced consistent cooling curves with similar values of the rodlet temperature at which the slope changes dramatically, in the range from 410°C to 430°C. The initial quenching test in alumina nanofluids showed a temperature history that is almost identical to that in the water tests. However, the quenching process in the subsequent repetitions with the alumina nanofluids was considerably accelerated, with rodlet temperatures at the transition point increasing up to 740°C (4^{th} run). On the other hand, the repetitions with *diamond* nanofluids did not display the same acceleration phenomenon, as shown in Fig. 2(c).

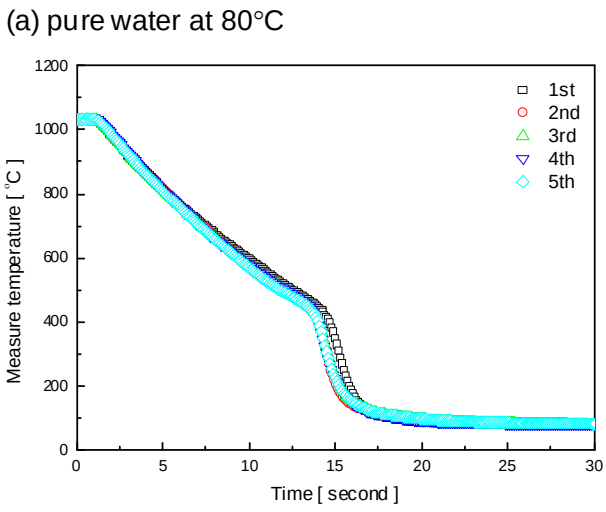

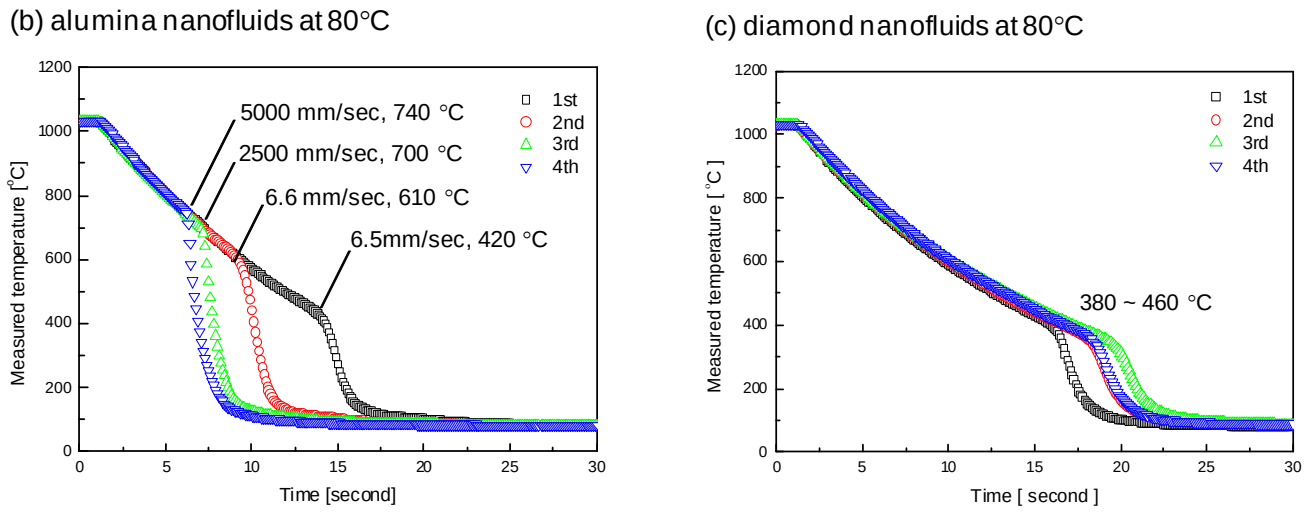

Figure 2 Temperature history of quenched rodlets.

(a) Water: t = 0, 1, 2, 3, 4, 5 sec; T_{rod} ~ 420 °C

(b) 1st run in alumina nanofluids: t = 0, 1, 2, 3, 4, 5 sec; T_{rod} ~ 420 °C

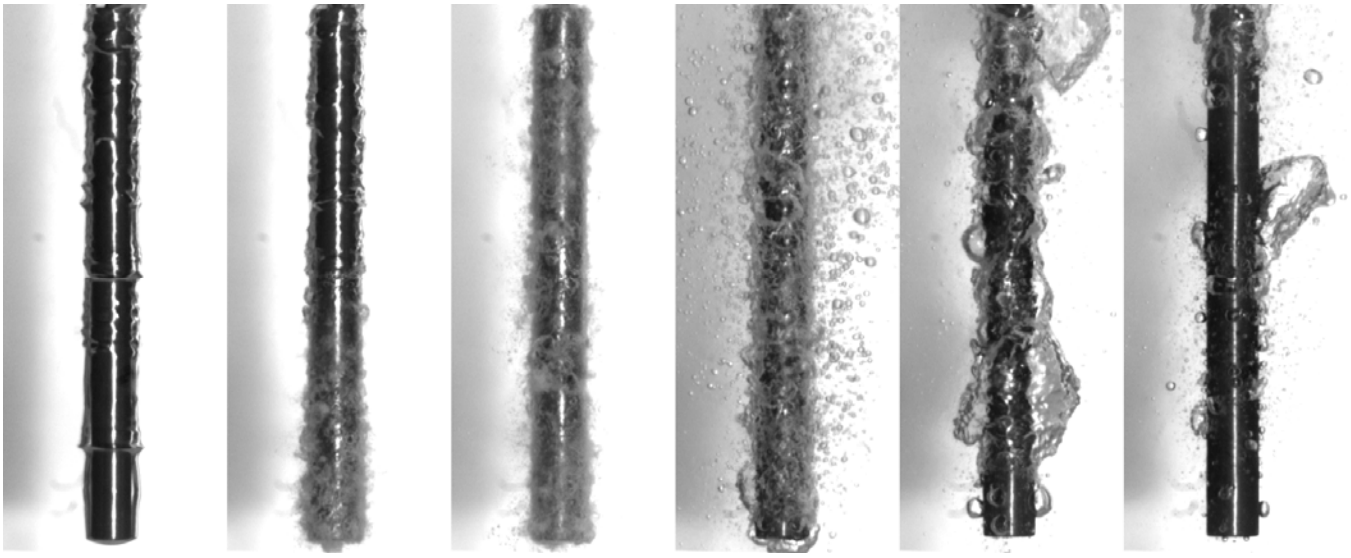

(c) 3rd run in alumina nanofluids: t = 0, 0.01, 0.02, 0.50, 1.00, 1.50 sec; T_{rod} ~ 700 °C

Figure 3 High-speed camera visualization of quenching phenomena for rodlets in pure water and alumina nanofliuids at 80°C.

Propagation of quench front

Quenching occurred through propagation of a quench front on the rodlet specimen for pure water and alumina nanofluids (Fig. 3). The edge of the quench front was characterized by a line of vigorous boiling. The quench front speeds were measured from the high-speed camera frames, and the values are reported in Fig. 2. With reference to Fig. 3(a), the stable vapor film started to collapse from the bottom of the rod at the rodlet temperature of 420 °C. The quench front moved up along the rod with a moving speed of 6.5-8.2 mm/sec. The initial quench front speed in alumina nanofluids was found to be ~7.2 mm/sec with an associated rodlet temperature of 420 °C, within the scattering range of the water tests. However, the subsequent test in nanofluids showed quite a different behavior. The vapor film started to collapse at much higher temperature, ~700 °C, and the quench front propagated at a much higher velocity, ~2.5 m/sec, which is about three orders of magnitude higher than the values for water. In fact, the quenching process was so fast, that the transition from film boiling to nucleate boiling seemed to occur almost simultaneously on the entire surface, as shown in Fig. 3(c). Unfortunately, the diamond nanofluid was too opaque to visualize the quench front.

Effect of nanoparticle deposition

It is well known that a nanoparticle deposition layer is formed on the boiling surface due to evaporation of nanofluids (Kim et al., 2007). This was observed also in our experiments. Since the accelerated quenching behavior observed in the alumina nanofluid tests is reproduced when an alumina-nanoparticle-fouled rodlet is quenched in pure water (6th test case in Fig. 4), it is clear that the nanoparticles deposited on the rodlet surface (not the nanoparticles dispersed in the nanofluid) are responsible for the accelerated quenching. With subsequent quenches in pure water, the quench front velocity gradually decreases again, which suggests that the particle deposition may be re-dispersed in water.

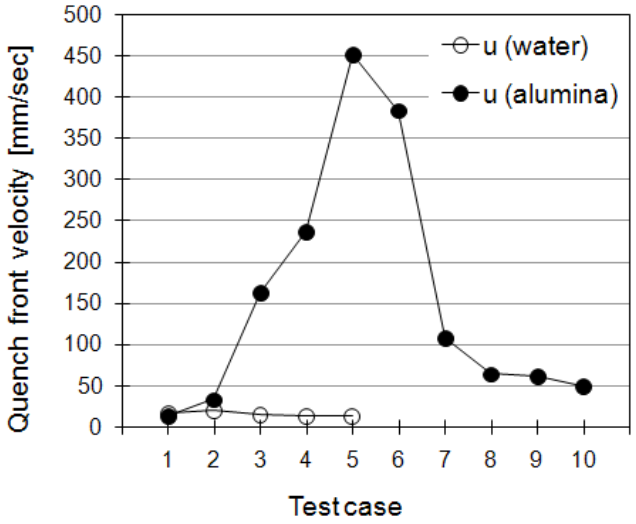

Figure 4 Quench front velocity of water and alumina at 30°C. 1-5: test in pure water or nanofluids; 6-10: tests in pure water for the rodlet previously quenched in tests 1-5.

DATA INTERPRETATION

The experimental results strongly point to the nanoparticle deposition on the surface to be responsible for the acceleration of the quenching process. In this section we discuss this effect in some detail.

When the hot rodlet and the cold liquid put in contact with each other, the instantaneous interface temperature assumes a value dictated by the thermal effusivities of the two materials (Carslaw and Jaeger, 1959),

$$T_{\text{int}} = \frac{T_w + \xi T_f}{1+\xi} \qquad \text{where} \quad \xi = \sqrt{\frac{k_f \rho_f c_f}{k_w \rho_w c_w}} \tag{1}$$

If this interfacial temperature is higher than the rewetting temperature for the fluid/rodlet pair, quenching cannot occur. The rewetting of the liquid on the heated surface is governed by the maximum allowable superheat of liquid near the interface at the moment of contact (Spiegler et al., 1963),

$$T_{\text{int}}\,(T_w = T_{\text{rew}},\, T_f) = T_{\text{MAX}} \tag{2}$$

Since the maximum allowable temperature depends on the physico-chemical properties of the surface, namely the wettability, Gerweck and Yadigaroglu (1992) suggested a wettability correction factor, f, to correlate the maximum allowable temperature with the critical temperature of the fluid, as shown below:

$$T_{\text{MAX}} \sim f\, T_C \tag{3}$$

where T_c is the critical temperature of the fluid, i.e., 374 °C for water. At T_{sat}=100 °C (T_{sat}/T_C = 0.58), f is found (Gerweck and Yadigaroglu, 1992) to be 0.81 and 0.89 for clean stainless steel surface ($\theta \sim 80°$) and alumina nanoparticle-fouled surface ($\theta \sim 15°$), respectively. The rewetting temperatures on these two surfaces are then calculated using Eqs. (1) ~ (3), and are 251°C for the clean stainless steel surface and 303°C for the alumina nanoparticle-fouled surface.

The calculated values of the rewetting temperature can be used to estimate the corresponding quench front velocity, using a simple quench front propagation model. It is traditionally assumed that the quench front velocity is controlled by axial heat conduction within the solid substrate in the narrow quench front region. An approximate analytical solution of the two-dimensional (r and z) quench front problem was derived by Duffey and Pothouse (1973), as given below:

For Bi << 1,

$$u^{-1} = \rho c \left(\frac{R}{2hk}\right)^{\frac{1}{2}} \frac{(T_{rod}-T_f)^{\frac{1}{2}}(T_{rod}-T_{rew})^{\frac{1}{2}}}{(T_{rew}-T_f)} \tag{4}$$

For Bi >> 1,

$$u^{-1} = \frac{\pi \rho c}{2h}\frac{(T_{rod}-T_f)}{(T_{rew}-T_f)}\left\{1-\frac{4}{\pi^2}Bi\frac{(T_{rew}-T_f)}{(T_{rod}-T_f)}\right\}^{\frac{1}{2}} \tag{5}$$

The density and specific heat in these equations are for the stainless steel rod. *Bi* in our study is about 3.7. Therefore, we can use Eq. (5) to estimate the quench front velocity. The boiling heat transfer coefficient, h, can vary from water to nanofluids, but the deviation is usually not very significant. For example, experiments performed in our laboratory showed that the nucleate boiling heat transfer coefficient of nanofluids is almost identical to that of water (Kim et al., 2009). Therefore, for this analysis a representative value of 5×10^4 W/m^2/K was assumed for both water and the nanofluids. The temperature of the rod (at the time of transition from film boiling to nucleate boiling), T_{rod}, is directly measured in our experiments, whereas the rewetting temperature is taken from the estimates at the beginning of this section. The temperature of the fluid is fixed at 80°C.

Table 1: Rewetting temperatures and quench front velocities

	T_f (°C)	T_{rod} (°C)	T_{rew} θ (°)	T_{rew} Eqs. (1~3)	h (W/m2-K)	Bi	u (mm/sec) Calculated by Eq. (5)	u (mm/sec) Measured from exp.
Water	80	420	80	251	50000	3.7	7.4	7.6
Alumina NF 1st test	80	420	80	251	50000	3.7	7.4	6.5
Alumina NF 4th test	80	750	15	303	50000	3.7	3.5	5000

Table 1 reports the values of the quench front velocity calculated by means of Eq. (5) for three representative cases. In spite of a higher rewetting temperature, the model of Eq. (5) predicts a reduction of the quench front velocity for the nanoparticle-fouled rodlet, mainly because the rod temperature for this case is very high. However, the experiments clearly show the opposite trend, i.e., the nanoparticle-fouled rodlet has a much higher quench front velocity. This led us to question the physical validity of the model. Therefore, we decided to conduct numerical simulations of the two-dimensional quench front propagation problem. Figure 5 shows the model for the simulation of the vapor film collapse. The Fourier equation for two-dimensional transient heat conduction was numerically solved for our rodlet geometry using the commercial code FLUENT® 6.0. To simulate the quenching process, the following assumptions were used for the convective heat transfer boundary conditions of the quenching surface:

For $T_w > T_{rew}$, h = 0 (film boiling region)
For $T_w \le T_{rew}$, h = 5×10^4 W/m^2/K. (nucleate boiling region)

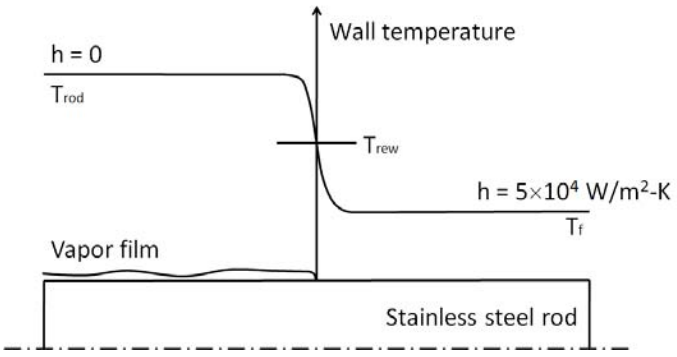

Figure 5 Model of the vapor film collapse used in simulation

The rod temperatures in the simulation were 420°C and 750°C, which were measured during our quenching experiments in pure water and the 4th alumina nanofluid tests, respectively. The 4th test in nanofluid actually exhibited the extremely high quench front velocity of ~ 5000 mm/sec.

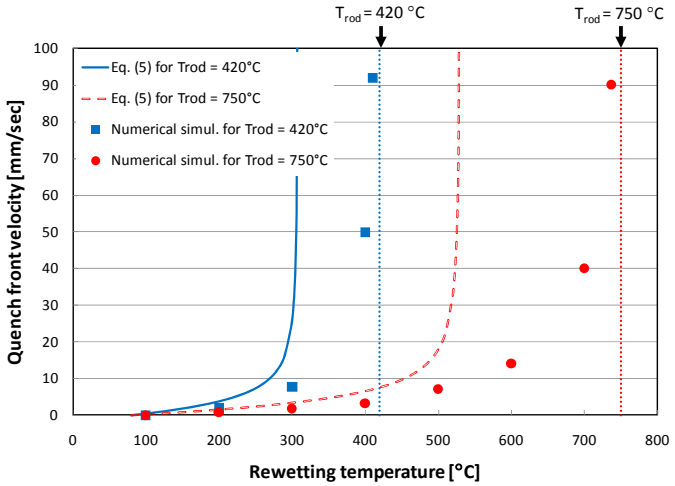

Figure 6 Numerical simulation results of quench front speed vs rewetting temperature.

Figure 6 shows the predictions of the numerical simulations, and compares them to the analytical solution of Duffey and Pothouse (1973). It is seen that the quench front velocity predicted by the numerical simulation is relatively low (and in good agreement with the analytical solution) when $T_{rew} << T_{rod}$. On the other hand, when the rewetting temperature approaches the rod temperature, $T_{rew} \rightarrow T_{rod}$, the quench front velocity becomes very high, i.e., in the limit comparable to the experimentally observed velocity. The problem is that such a high rewetting temperature (420-750°C) is not physically possible, as it is well above the critical temperature of water (374°C). Therefore, we can conclude that the very high quench front speed is not compatible with the notion of a quench front that is controlled by axial heat conduction within the rodlet.

CONCLUSIONS AND FUTURE WORKS

Conclusions of this study are as follows:

1. The nanoparticles dispersed in the fluid at low concentration (< 0.1 v%) do not change the quenching process appreciably.
2. The nanoparticles that deposit on the rodlet surface may accelerate the quenching process very significantly, up to three orders of magnitude in terms of quench front propagation velocity, and up to 750°C in terms of temperature at which the transition to nucleate boiling begins. The acceleration strongly depends on the nanoparticle material used, i.e., the alumina nanoparticles on the surface significantly improve the quenching, while the diamond nanoparticles do not.
3. Vapor film collapse in the accelerated quench tests does not seem to be controlled by axial heat conduction in the rodlet.

Further investigation and quantification of the quench acceleration mechanism in the presence of nanoparticle deposition is underway. The results will be presented in a future publication.

ACKNOWLEDGMENTS

This research was supported by AREVA, a generous gift from Mr. Doug Spreng, and the Korea Research Foundation Grant funded by the Korean Government (MOEHRD) (KRF-2007-357-D00026).

REFERENCES

1. Bang, I. C., and Chang, S. H., 2005, "Boiling heat transfer performance and phenomena of Al_2O_3-water nano-fluids from a plain surface in a pool," *Int. J. Heat and Mass Transfer*, **48**, pp. 2407-2419.
2. Berenson, P. J., 1961, "Film boiling heat transfer from a horizontal surface," *J. Heat Transfer*, **83C**, pp. 351-358.
3. Carslaw, H., Jaeger, J., 1959, *Heat conduction in solids* (2nd Edn), Clarendon Press, Oxford.
4. Choo, Y. J., Chun, S. Y., Park, J. K., Song, C. H., Bang, I. C., 2008, "Experimental Study on Boiling Heat Transfer using Standard Nanofluids," *Proc. the 7th International Topical Meeting on Nuclear Reactor Thermal Hydraulics, Operation and Safety*, Seoul, Korea.
5. Duffey, R. B., Porthouse, D. T. C., 1973, "The physics of rewetting in water reactor emergency core cooling" *Nucl. Eng. Design*, **25**, pp. 379-394.
6. Gerwreck, V., Yadigaroglu, G., 1992, "A local equation of state for a fluid in the presence of a wall and its application to rewetting," *Int. J. Heat and Mass Transfer*, **35**, pp. 1823–1832.
7. Henry, R. E., 1974, "A correlation for the minimum film boiling temperature," *A.I.Ch.E. Symposium Series*, **70**, pp. 81-90.
8. Kim, H. D., Kim, J. B., and Kim, M. H., 2006, "Effect of nanoparticles on CHF enhancement in pool boiling of nanofluids," *Int. J. Heat and Mass Transfer*, **49**, pp. 5070-5074.
9. Kim, H. D., Buongiorno, J., Hu, L. W., McKrell, T., DeWitt, G., 2008, "Experimental study on quenching of a small metal sphere in nanofluids," *Proc. ASME International Mechanical Engineering Congress and Exposition*, Boston, USA.
10. Kim, H. D., DeWitt, McKrell, T., G., Buongiorno, J., Hu, L. W., "On the Quenching of Steel and Zircaloy Spheres in Water-Based Nanofluids with Alumina, Silica and Diamond Nanoparticles," *Int. J. Multiphase Flow,* (submitted).
11. Kim, S. J., Bang, I. C., Buongiorno, J., and Hu, L. W., 2007, "Surface wettability change during pool boiling of nanofluids and its effect on critical heat flux," *Int. J. Heat and Mass Transfer*, **50**, pp. 4105–4116.
12. Ohtake, H., Koizumi, Y., 2004, "Study on propagative collapse of a vapor film in film boiling (mechanism of vapor-film collapse at wall temperature above the thermodynamic limit of liquid superheat)," *Int. J. Heat and Mass Transfer*, **47**, pp. 1965–1977.
13. Park, H. S., Shiferaw, D., Sehgal, B. R., Kim, D. K., and Muhammed, M., 2004, "Film boiling heat transfer on a high temperature sphere in nanofluid," *Proc. ASME Heat Transfer/Fluids Engineering Summer Conference*, Charlotte, USA.
14. Spiegler, P., Hopenfeld, J., Silberberg, M., 1963, "Onset of stable film boiling and the foam limit," *Int. J. Heat and Mass Transfer*, **6**, pp. 987-989.
15. Vassallo, P., Kumar, R., and D'Amico, S., 2004, "Pool boiling heat transfer experiments in silica-water nanofluids," *Int. J. Heat and Mass Transfer*, **47**, pp. 407-411.
16. Xue H. S., J. R. Fan, R. H. Hong, Y. C. Hu, 2007, "Characteristic boiling curve of carbon nanotube nanofluid as determined by the transient calorimeter technique," *Appl. Phys. Letter*, **90**, 184107.
17. You, S. M., Kim, J. H., and Kim, K. H., 2003, "Effects of nanoparticles on critical heat flux of water in pool boiling heat transfer," *Appl. Phys. Lett.*, **83**, pp. 3374-3376.

